

# Learning Hierarchical Protein Representations via Complete 3D Graph Networks

ICLR 2023

Limei Wang\*, Haoran Liu\*, et al.

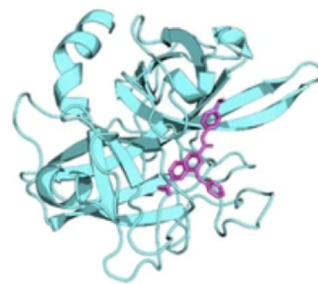
Texas A&M University

## Protein representation

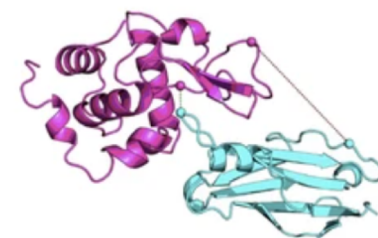
- ▶ Learn representations of proteins with 3D structures
  - ▶ Learning representations for various downstream tasks
  - ▶ Challenges: how to capture protein structures efficiently?
- ▶ The paper verifies that different tasks focus on different representations, such as backbone, all atoms, side chains.



Protein structure ranking  
Enzyme reaction prediction



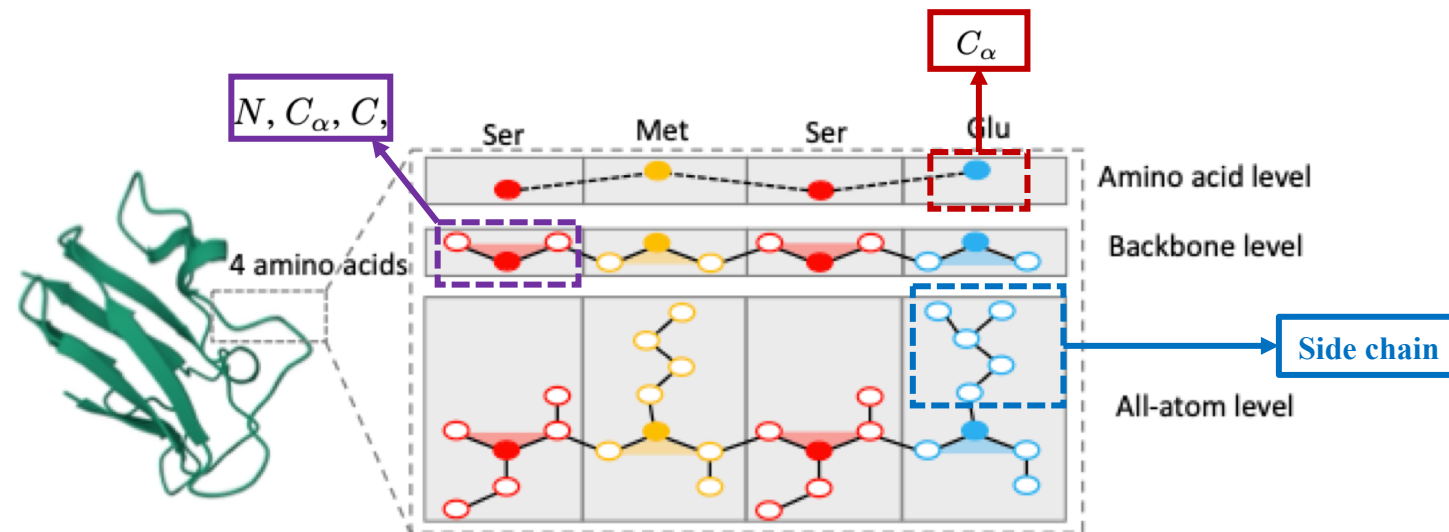
Ligand binding affinity



Protein-protein interfaces

## Protein structure

- ▶ Proteins are highly complex macromolecules
  - ▶ Hundreds or even thousands of amino acids
  - ▶ An amino acid contains a detailed inner structure: Nitrogen(N), Carbon(C)
  - ▶ Treat each amino acid instead of each atom as a node, use a radial cutoff to construct edges



## GNNs for proteins

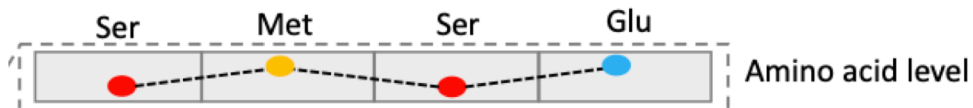
Denotations:

- ▶ A 3D graph:  $G = (\mathcal{V}, \mathcal{E}, \mathcal{P})$ 
  - ▶  $\mathcal{V} = \{\mathbf{v}_i\}_{i=1,\dots,n}$  is the set of node features;
  - ▶  $\mathcal{E} = \{\mathbf{e}_{ij}\}_{i,j=1,\dots,n}$  is the set of edge features;
  - ▶  $\mathcal{P} = \{P_i\}_{i=1,\dots,n}$  is the set of position matrices, where  $P_i \in \mathbb{R}^{k_i \times 3}$  ;

Message passing:

$$\mathbf{v}_i^{l+1} = \text{UPDATE} \left( \mathbf{v}_i^l, \sum_{j \in \mathcal{N}_i} \text{MESSAGE} \left( \mathbf{v}_j^l, \mathbf{e}_{ji}, \boxed{\mathcal{F}(G)} \right) \right) \rightarrow \text{Geometric Representations}$$

## Geometric Representations: Amino Acid level



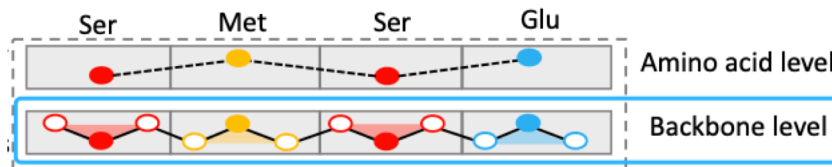
Geometric representation[1]:

$$\mathcal{F}(\mathbf{G})_{\text{base}} = \{\mathbf{d}_{ij}, \theta_{ij}, \phi_{ij}, \tau_{ij}\}_{i=1, \dots, n, j \in N_i} \quad (1)$$

- ▶  $\mathbf{d}_{ij}, \theta_{ij}, \phi_{ij}$ , is the spherical coordinate of node  $j$  in the local coordinate system (LCS) of node  $i$  ;
- ▶ LCS of  $i$  : based on nodes  $i$ ,  $i - 1$ , and  $i + 1$
- ▶  $\tau_{ij}$  is the rotation angle of edge  $ij$

[1] Wang, Limei, et al. “ComENet: towards complete and efficient message passing for 3D molecular graphs.” NeurIPS 2022.

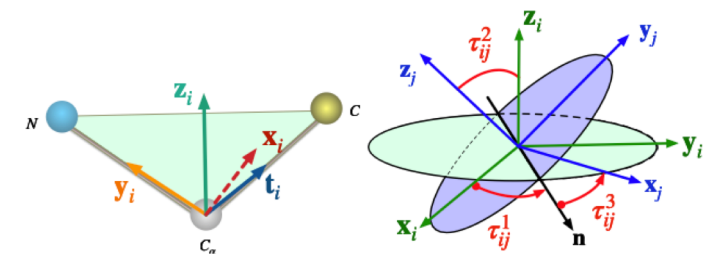
## Geometric Representations: Backbone level



Geometric representation:

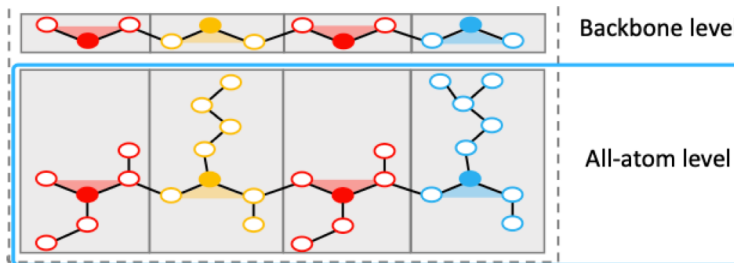
$$\mathcal{F}(G)_{bb} = \underbrace{\{d_{ij}, \theta_{ij}, \phi_{ij}, \tau_{ij}\}}_{\mathcal{F}(G)_{base}} \cup \{(\tau_{ji}^1, \tau_{ji}^2, \tau_{ji}^3)\}_{i=1, \dots, n, j \in N_i} \quad (2)$$

- ▶ Treat the backbone structure as rigid triangles; [2]
- ▶ Only degree of freedom: relations between rigid triangles;
- ▶ Use Euler angles to explicitly capture such information;



[2] Jumper, John, et al. "Highly accurate protein structure prediction with AlphaFold" Nature 596.7873 (2021): 583-589

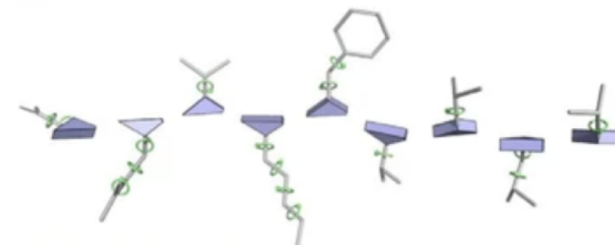
## Geometric Representations: All-atom level



Geometric representation:

$$\mathcal{F}(\mathbf{G})_{\text{all}} = \underbrace{\{d_{ij}, \theta_{ij}, \phi_{ij}, \tau_{ij}\}}_{\mathcal{F}(\mathbf{G})_{\text{bb}}} \cup \{(\tau_{ji}^1, \tau_{ji}^2, \tau_{ji}^3)\} \cup \{\mathcal{X}_i^1, \mathcal{X}_i^2, \mathcal{X}_i^3, \mathcal{X}_i^4\}_{i=1, \dots, n, j \in N_i} \quad (3)$$

- ▶ Assume all bond lengths and bond angles in each amino acid are fully rigid; [3]
- ▶ Only degree of freedom for each amino acid: Side chain torsion angles;
- ▶ At most five torsion angles for any amino acid;



[2] Jumper, John, et al. "Highly accurate protein structure prediction with AlphaFold" Nature 596.7873 (2021): 583-589

## Geometric Representations: All-atom level

- ▶ Atoms for computing the side chain torsion angles for each amino acid

Table 7: Atoms for computing the side chain torsion angles for each amino acid.

	$\chi^1$	$\chi^2$	$\chi^3$	$\chi^4$	$\chi^5$
ALA					
ARG	$N, C_\alpha, C_\beta, C_\gamma$	$C_\alpha, C_\beta, C_\gamma, C_\delta$	$C_\beta, C_\gamma, C_\delta, N_\epsilon$	$C_\gamma, C_\delta, N_\epsilon, C_\zeta$	$C_\delta, N_\epsilon, C_\zeta, N_{\eta 1}$
ASN	$N, C_\alpha, C_\beta, C_\gamma$	$C_\alpha, C_\beta, C_\gamma, O_{\delta 1}$			
ASP	$N, C_\alpha, C_\beta, C_\gamma$	$C_\alpha, C_\beta, C_\gamma, O_{\delta 1}$			
CYS	$N, C_\alpha, C_\beta, S_\gamma$				
GLN	$N, C_\alpha, C_\beta, C_\gamma$	$C_\alpha, C_\beta, C_\gamma, C_\delta$	$C_\beta, C_\gamma, C_\delta, O_{\epsilon 1}$		
GLU	$N, C_\alpha, C_\beta, C_\gamma$	$C_\alpha, C_\beta, C_\gamma, C_\delta$	$C_\beta, C_\gamma, C_\delta, O_{\epsilon 1}$		
GLY					
HIS	$N, C_\alpha, C_\beta, C_\gamma$	$C_\alpha, C_\beta, C_\gamma, N_{\delta 1}$			
ILE	$N, C_\alpha, C_\beta, C_{\gamma 1}$	$C_\alpha, C_\beta, C_{\gamma 1}, C_{\delta 1}$			
LEU	$N, C_\alpha, C_\beta, C_\gamma$	$C_\alpha, C_\beta, C_\gamma, C_{\delta 1}$			
LYS	$N, C_\alpha, C_\beta, C_\gamma$	$C_\alpha, C_\beta, C_\gamma, C_\delta$	$C_\beta, C_\gamma, C_\delta, C_\epsilon$	$C_\gamma, C_\delta, C_\epsilon, N_\zeta$	
MET	$N, C_\alpha, C_\beta, C_\gamma$	$C_\alpha, C_\beta, C_\gamma, S_\delta$	$C_\beta, C_\gamma, S_\delta, C_\epsilon$		
PHE	$N, C_\alpha, C_\beta, C_\gamma$	$C_\alpha, C_\beta, C_\gamma, C_{\delta 1}$			
PRO	$N, C_\alpha, C_\beta, C_\gamma$	$C_\alpha, C_\beta, C_\gamma, C_\delta$			
SER	$N, C_\alpha, C_\beta, O_\gamma$				
THR	$N, C_\alpha, C_\beta, O_{\gamma 1}$				
TRP	$N, C_\alpha, C_\beta, C_\gamma$	$C_\alpha, C_\beta, C_\gamma, C_{\delta 1}$			
TYR	$N, C_\alpha, C_\beta, C_\gamma$	$C_\alpha, C_\beta, C_\gamma, C_{\delta 1}$			
VAL	$N, C_\alpha, C_\beta, C_{\gamma 1}$				

# Geometric Representations: specific calculation method

## C.1 GEOMETRIC REPRESENTATIONS

The geometric representation at the amino acid level is  $\mathcal{F}(G)_{\text{base}} = \{(d_{ji}, \theta_{ji}, \phi_{ji}, \tau_{ji})\}_{i=1, \dots, n, j \in N_i}$  as introduced in Sec. [3.1]. For each edge  $ji$ , we need to compute four geometries based on the positions of nodes  $i, j, i - 1, i + 1, j - 1$  and  $j + 1$ . We use  $\mathbf{p}_i^1, \mathbf{p}_i^2, \mathbf{p}_{ij}, \mathbf{p}_j^1, \mathbf{p}_j^2$  to denote the unit vectors of  $\mathbf{r}_{i-1} - \mathbf{r}_i, \mathbf{r}_{i+1} - \mathbf{r}_i, \mathbf{r}_j - \mathbf{r}_i, \mathbf{r}_{j-1} - \mathbf{r}_j$  and  $\mathbf{r}_{j+1} - \mathbf{r}_j$ . Then the four geometries for edge  $ji$  are computed based on

$$\begin{aligned} d_{ji} &= \|\mathbf{p}_{ij}\|_2, \\ \theta_{ji} &= \arccos(\mathbf{p}_i^1 \cdot \mathbf{p}_{ij}), \\ \mathbf{n}_1 &= \mathbf{p}_i^1 \times \mathbf{p}_i^2, \quad \mathbf{n}_2 = \mathbf{p}_i^1 \times \mathbf{p}_{ij}, \\ \phi_{ji} &= \text{atan2}(\mathbf{n}_1 \cdot \mathbf{n}_2, \mathbf{n}_1 \times \mathbf{n}_2), \\ \mathbf{p}_i &= \begin{cases} \mathbf{p}_i^2, & \text{if } j = i - 1 \\ \mathbf{p}_i^1, & \text{otherwise} \end{cases}, \quad \mathbf{p}_j = \begin{cases} \mathbf{p}_j^2, & \text{if } i = j - 1 \\ \mathbf{p}_j^1, & \text{otherwise} \end{cases}, \\ \mathbf{n}_3 &= \mathbf{p}_{ij} \times \mathbf{p}_i, \quad \mathbf{n}_4 = \mathbf{p}_{ij} \times \mathbf{p}_j, \\ \tau_{ji} &= \text{atan2}(\mathbf{n}_3 \cdot \mathbf{n}_4, \mathbf{n}_3 \times \mathbf{n}_4). \end{aligned} \tag{21}$$

As introduced in Sec. [3.2], the geometric representation at the backbone level is

$$\begin{aligned} \mathcal{F}(G)_{\text{bb}} &= \mathcal{F}(G)_{\text{base}} \cup \{(\tau_{ji}^1, \tau_{ji}^2, \tau_{ji}^3)\}_{i=1, \dots, n, j \in N_i} \\ &= \{(d_{ji}, \theta_{ji}, \phi_{ji}, \tau_{ji})\}_{i=1, \dots, n, j \in N_i} \cup \{(\tau_{ji}^1, \tau_{ji}^2, \tau_{ji}^3)\}_{i=1, \dots, n, j \in N_i} \\ &= \{(d_{ji}, \theta_{ji}, \phi_{ji}, \tau_{ji}, \tau_{ji}^1, \tau_{ji}^2, \tau_{ji}^3)\}_{i=1, \dots, n, j \in N_i}. \end{aligned} \tag{22}$$

The steps to compute the Euler angles  $\tau^1, \tau^2, \tau^3$  are provided in Sec. [3.2] and Fig. [2].

As introduced in Sec. [3.3], the geometric representation at the all-atom level is

$$\begin{aligned} \mathcal{F}(G)_{\text{all}} &= \mathcal{F}(G)_{\text{bb}} \cup \{(\chi_i^1, \chi_i^2, \chi_i^3, \chi_i^4)\}_{i=1, \dots, n} \\ &= \{(d_{ji}, \theta_{ji}, \phi_{ji}, \tau_{ji}, \tau_{ji}^1, \tau_{ji}^2, \tau_{ji}^3)\}_{i=1, \dots, n, j \in N_i} \cup \{(\chi_i^1, \chi_i^2, \chi_i^3, \chi_i^4)\}_{i=1, \dots, n}. \end{aligned} \tag{23}$$

The atoms used to compute the side chain torsion angles  $\chi^1, \chi^2, \chi^3, \chi^4$  are provided in Table [7].

## ► Amino Acid level

$$\mathcal{F}(G)_{\text{base}} = \{\mathbf{d}_{ij}, \theta_{ij}, \phi_{ij}, \tau_{ij}\}_{i=1, \dots, n, j \in N_i}$$

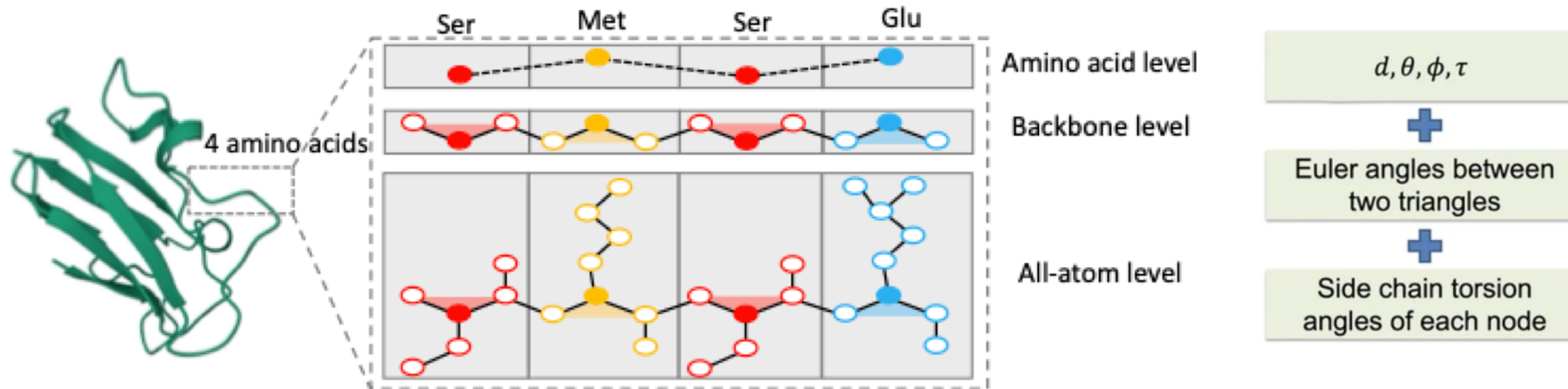
## ► Backbone level

$$\mathcal{F}(G)_{\text{bb}} = \underbrace{\{\mathbf{d}_{ij}, \theta_{ij}, \phi_{ij}, \tau_{ij}\}}_{\mathcal{F}(G)_{\text{base}}} \cup \{(\tau_{ji}^1, \tau_{ji}^2, \tau_{ji}^3)\}_{i=1, \dots, n, j \in N_i}$$

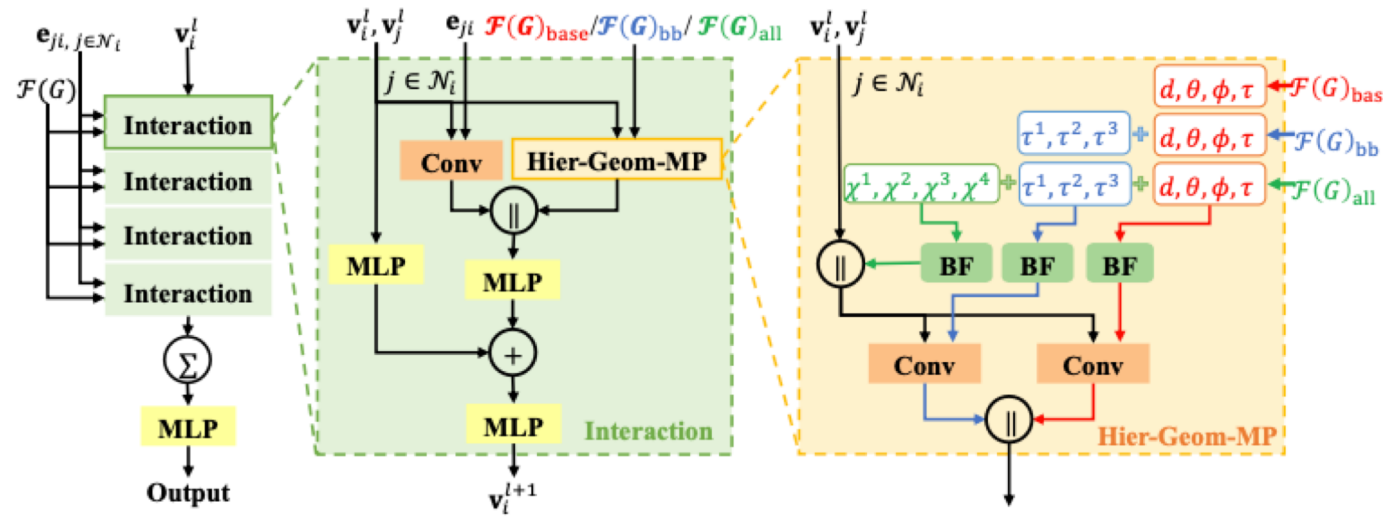
## ► All-atom level

$$\mathcal{F}(G)_{\text{all}} = \underbrace{\{\mathbf{d}_{ij}, \theta_{ij}, \phi_{ij}, \tau_{ij}\}}_{\mathcal{F}(G)_{\text{bb}}} \cup \{(\tau_{ji}^1, \tau_{ji}^2, \tau_{ji}^3)\} \cup \{\chi_i^1, \chi_i^2, \chi_i^3, \chi_i^4\}_{i=1, \dots, n, j \in N_i}$$

► Comparisons between three geometric representations



# ProNet Framework



ProNet-Amino Acid

ProNet-Backbone

ProNet-All- Atom

- The message passing scheme:

$$\mathbf{v}_i^{l+1} = \text{UPDATE} \left( \mathbf{v}_i^l, \sum_{j \in \mathcal{N}_i} \text{MESSAGE} (\mathbf{v}_j^l, \mathbf{e}_{ji}, \mathcal{F}(G)) \right)$$

- The three levels of geometric representations result in three levels of ProNet, namely **ProNet-Amino Acid**, **ProNet-Backbone**, and **ProNet-All- Atom**. (Concatenate features)
- Users can easily adapt the framework to different downstream tasks by specifying the level of geometric representations

## Comparisons of different all-atom methods

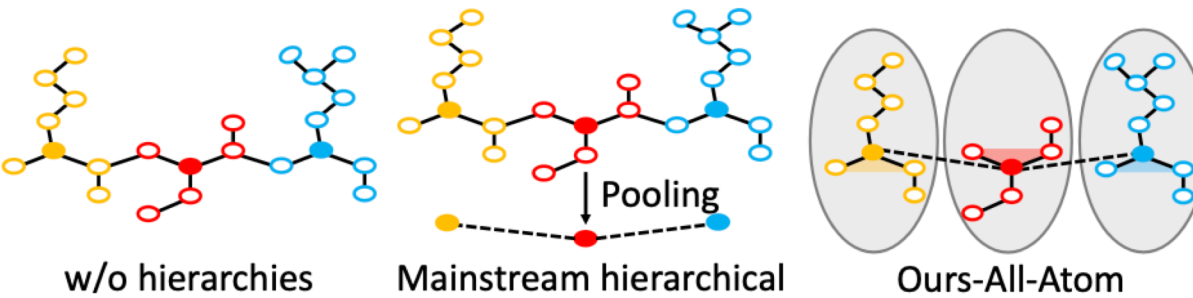


Figure 3: Illustrations of three kind of all-atom level methods.

- ▶ The vector-gated GVP-GNN belongs to the "w/o hierarchies" methods. It treats each atom as a node and uses an equivariant GNN to update node features.
- ▶ IEConv follows the "mainstream hierarchical" methods. It treats each atom as a node and uses several pooling layers to obtain representations at different levels, which induces excessive computing costs.
- ▶ In addition, by treating each amino acid as a node and integrating side chain torsion angles as node features, our method has much fewer nodes in constructed graphs, **resulting in a much more efficient learning framework**.

## Experiments: Reaction Classification and Fold Classification

Table 2: Accuracy (%) on fold and reaction classification tasks. The top two results are highlighted as **1st** and **2nd**.

Method	React	Fold			
		Fold	Sup.	Fam.	Avg.
GCN (Kipf & Welling, 2017)	67.3	16.8	21.3	82.8	40.3
DeepSF (Hou et al., 2018)	70.9	17.0	31.0	77.0	41.7
GVP-GNN (Jing et al., 2021b)	65.5	16.0	22.5	83.8	40.8
IEConv (Hermosilla et al., 2021)	<b>87.2</b>	45.0	69.7	98.9	71.2
New IEConv (Hermosilla & Ropinski, 2022)	<b>87.2</b>	47.6	<u>70.2</u>	99.2	72.3
HoloProt (Somnath et al., 2021)	78.9	—	—	—	—
DWNN (Li et al., 2022)	76.7	31.8	37.8	85.2	51.5
GearNet (Zhang et al., 2023)	79.4	28.4	42.6	95.3	55.4
GearNet-IEConv (Zhang et al., 2023)	83.7	42.3	64.1	99.1	68.5
GearNet-Edge (Zhang et al., 2023)	<u>86.6</u>	44.0	66.7	99.1	69.9
GearNet-Edge-IEConv (Zhang et al., 2023)	85.3	48.3	<b>70.3</b>	<b>99.5</b>	72.7
ProNet-Amino Acid	86.0	51.5	69.9	99.0	73.5
ProNet-Backbone	86.4	<b>52.7</b>	<b>70.3</b>	<u>99.3</u>	<b>74.1</b>
ProNet-All-Atom	85.6	<u>52.1</u>	69.0	99.0	73.4

### ► Fold Dataset:

In this task, 12,312 proteins are used for training, 736 for validation, 718 for Fold, 1,254 for Superfamily, and 1,272 for Family.

### ► Reaction Dataset:

The dataset is split into 29,215 proteins for training, 2,562 for validation, and 5,651 for testing.

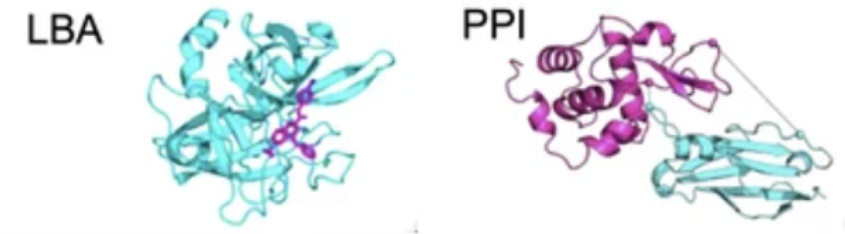
► Table shows that our methods can achieve the best results on two of the three test sets and the best average value;

► ProNet-backbone performs better;

► GearNet method: without pretraining

## Result: LBA and PPI

Method	Sequence Identity 30%			Sequence Identity 60%		
	RMSE ↓	Pearson ↑	Spearman ↑	RMSE ↓	Pearson ↑	Spearman ↑
Atom3D-3DCNN* (Townshend et al., 2021)	<b>1.416</b>	0.550	<b>0.553</b>	1.621	0.608	0.615
Atom3D-ENN* (Townshend et al., 2021)	1.568	0.389	0.408	1.620	0.623	0.633
Atom3D-GNN* (Townshend et al., 2021)	1.601	0.545	0.533	1.408	0.743	0.743
DeepDTA (Öztürk et al., 2018)	1.866	0.472	0.471	1.762	0.666	0.663
Bepler and Berger (2019) (Bepler & Berger, 2019)	1.985	0.165	0.152	1.891	0.249	0.275
TAPE (Rao et al., 2019)	1.890	0.338	0.286	1.633	0.568	0.571
ProtTrans (Elnaggar et al., 2021)	1.544	0.438	0.434	1.641	0.595	0.588
MaSIF (Gainza et al., 2020)	1.484	0.467	0.455	1.426	0.709	0.701
IEConv (Hermosilla et al., 2021)	1.554	0.414	0.428	1.473	0.667	0.675
Holoprot-Full Surface (Somnath et al., 2021)	1.464	0.509	0.500	1.365	0.749	0.742
Holoprot-Superpixel (Somnath et al., 2021)	1.491	0.491	0.482	1.416	0.724	0.715
ProNet-Amino Acid	<b>1.455</b>	0.536	0.526	1.397	0.741	0.734
ProNet-Backbone	1.458	0.546	0.550	<b>1.349</b>	<b>0.764</b>	<b>0.759</b>
ProNet-All-Atom	1.463	<b>0.551</b>	<b>0.551</b>	<b>1.343</b>	<b>0.765</b>	<b>0.761</b>



Method	AUROC ↑
Atom3D-3DCNN (Townshend et al., 2021)	0.844
Atom3D-GNN (Townshend et al., 2021)	0.669
GVP-GNN (Jing et al., 2021a)	<b>0.866</b>
ProNet-Amino Acid	0.857
ProNet-Backbone	0.858
ProNet-All-Atom	<b>0.871</b>

- ▶ ProNet-All-Atom performs better;
- ▶ LBA Dataset:  
The curated dataset of 3,507 complexes is split into train/val/test splits based on a 30% or 60% sequence identity threshold to verify the model generalization ability for unseen proteins;
- ▶ PPI Dataset:  
We use the Database of Interacting Protein Structures (DIPS) for training and make prediction on the Docking Benchmark 5 (DB5);
- ▶ This is easy to understand because the interaction task is related to side chains.

## Observations:

- ▶ Different downstream tasks may require methods at different levels
  - ▶ On two function prediction tasks: **ProNet-backbone** performs better;
  - ▶ On two interaction prediction tasks: **ProNet-All-Atom** performs better;

## Efficiency Comparisons :

- ▶ More efficiency than baseline methods using the same GPU

Table 3: Comparisons between ProNet and other methods in terms of computational cost on the Fold dataset using the same Nvidia GeForce RTX 2080 Ti 11GB GPU.

Method	Hierarchical Level	Time (sec.)		Converge Time
		Train	Inference	
GearNet-Edge (Zhang et al., 2023)	Amino Acid	OOM	—	—
GearNet-Edge-IEConv (Zhang et al., 2023)	Amino Acid	OOM	—	—
GVP-GNN (Jing et al., 2021b)	Backbone	35	6	~ 9 h
IEConv (Hermosilla et al., 2021)	All-Atom	165	22	~ 24 h
ProNet-Amino Acid	Amino Acid	32	5	~ 9 h
ProNet-Backbone	Backbone	32	6	~ 9 h
ProNet-All-Atom	All-Atom	32	6	~ 9 h

## Conclusion:

- ▶ Hierarchical Protein Representations
  - ▶ Amino Acid level
  - ▶ Backbone level
  - ▶ All-atom level
- ▶ Different downstream tasks may require methods at different levels
  - ▶ On two function prediction tasks: ProNet-backbone performs better;
  - ▶ On two interaction prediction tasks: ProNet-All-Atom performs better;
- ▶ Without pretraining

w/o pretraining	Method	Pretraining Dataset (Size)	EC	GO			Fold Classification				Reaction
				BP MF CC			Fold	Super.	Fam.	Avg.	
				0.244	0.354	0.287	11.3	13.4	53.4	26.0	51.7
CNN (Shanehsazzadeh et al., 2020)	-	0.545	0.244	0.354	0.287	11.3	13.4	53.4	26.0	24.1	
ResNet (Rao et al., 2019)	-	0.605	0.280	0.405	0.304	10.1	7.21	23.5	13.6	11.0	
LSTM (Rao et al., 2019)	-	0.425	0.225	0.321	0.283	6.41	4.33	18.1	9.61	26.6	
Transformer (Rao et al., 2019)	-	0.238	0.264	0.211	0.405	9.22	8.81	40.4	19.4		
GCN (Kipf & Welling, 2017)	-	0.320	0.252	0.195	0.329	16.8*	21.3*	82.8*	40.3*	67.3*	
GAT (Veličković et al., 2018)	-	0.368	0.284†	0.317†	0.385†	12.4	16.5	72.7	33.8	55.6	
GVP (Jing et al., 2021)	-	0.489	0.326†	0.426†	0.420†	16.0	22.5	83.8	40.7	65.5	
3DCNN_MQA (Derevyanko et al., 2018)	-	0.077	0.240	0.147	0.305	31.6*	45.4*	92.5*	56.5*	72.2*	
GraphQA (Baldassarre et al., 2021)	-	0.509	0.308	0.329	0.413	23.7*	32.5*	84.4*	46.9*	60.8*	
New IEConv (Hermosilla & Ropinski, 2022)	-	0.735	0.374	0.544	0.444	47.6*	70.2*	99.2*	72.3*	87.2*	
GearNet	-	0.730	0.356	0.503	0.414	28.4	42.6	95.3	55.4	79.4	
GearNet-IEConv	-	0.800	0.381	0.563	0.422	42.3	64.1	99.1	68.5	83.7	
GearNet-Edge	-	<b>0.810</b>	<b>0.403</b>	<b>0.580</b>	<b>0.450</b>	44.0	66.7	99.1	69.9	86.6	
GearNet-Edge-IEConv	-	<b>0.810</b>	<b>0.400</b>	<b>0.581</b>	0.430	<b>48.3</b>	<b>70.3</b>	<b>99.5</b>	<b>72.7</b>	85.3	
DeepFRI (Gligorijević et al., 2021)	Pfam (10M)	0.631	0.399	0.465	0.460	15.3*	20.6*	73.2*	36.4*	63.3*	
ESM-1b (Rives et al., 2021)	UniRef50 (24M)	0.864	0.452	<b>0.657</b>	0.477	26.8	60.1	97.8	61.5	83.1	
ProtBERT-BFD (Elnaggar et al., 2021)	BFD (2.1B)	0.838	0.279†	0.456†	0.408†	26.6*	55.8*	97.6*	60.0*	72.2*	
LM-GVP (Wang et al., 2022b)	UniRef100 (216M)	0.664	0.417†	0.545†	<b>0.527†</b>	-	-	-	-	-	
New IEConv (Hermosilla & Ropinski, 2022)	PDB (476K)	-	-	-	-	50.3*	<b>80.6*</b>	99.7*	76.9*	87.6*	
Residue Type Prediction	AlphaFoldDB (805K)	0.843	0.430	0.604	0.465	48.8	71.0	99.4	73.0	86.6	
Distance Prediction	AlphaFoldDB (805K)	0.839	0.448	0.616	0.464	50.9	73.5	99.4	74.6	<b>87.5</b>	
Angle Prediction	AlphaFoldDB (805K)	0.853	0.458	0.625	0.473	<b>56.5</b>	76.3	99.6	77.4	86.8	
Dihedral Prediction	AlphaFoldDB (805K)	0.859	0.458	0.626	0.465	51.8	77.8	99.6	75.9	87.0	
Multiview Contrast	AlphaFoldDB (805K)	<b>0.874</b>	<b>0.490</b>	<b>0.654</b>	0.488	54.1	<b>80.5</b>	<b>99.9</b>	<b>78.1</b>	87.5	

The improvement in performance is obvious.

Thanks! Q&A